

Supplement of

Stochastically perturbed physics-tendencies based ensemble mean approach in the WRF model: a study for the North Indian Ocean tropical cyclones

5 Gaurav Tiwari, Vishal Bobde, Pankaj Kumar, and Alok Kumar Mishra

Department of Earth and Environmental Sciences,
Indian Institute of Science Education and Research Bhopal, Bhauli-462066, India

Correspondence to: Pankaj Kumar (kumarp@iiserb.ac.in)

10 **S1 Study domain**

S1.1 Arabian Sea (ARB)

For the simulation of ESCS Tauktae over the ARB, the WRF model was configured over a domain with dimensions 50°E-85°E, 5°S to 30°N as shown in Figure S1.

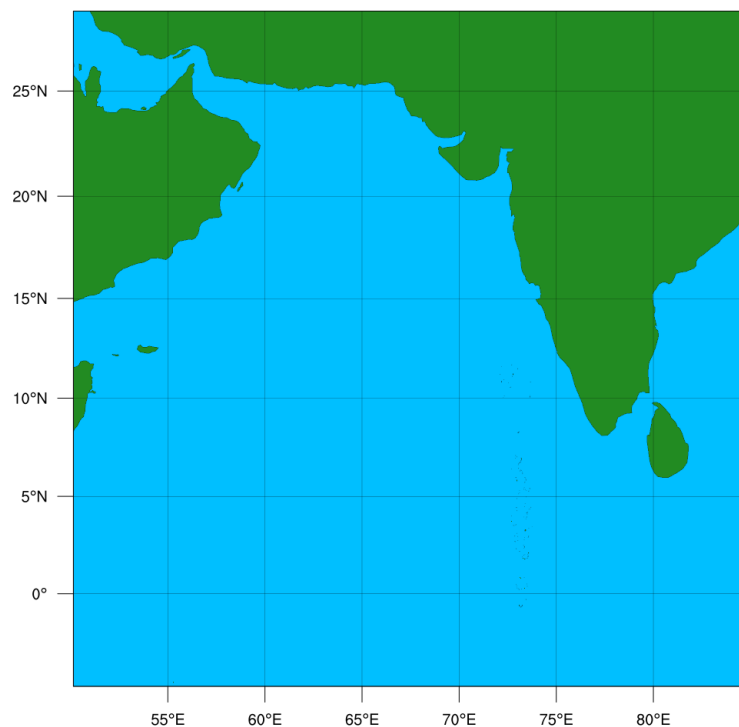


Figure S1: Study domain over the ARB for cyclone Tauktae.

S1.2 Bay of Bengal (BoB)

15 For the simulation of VSCS Nivar over the BoB, the WRF model was configured over a domain with dimensions 70°E-100°E, 2°S to 26°N as shown in Figure S2.

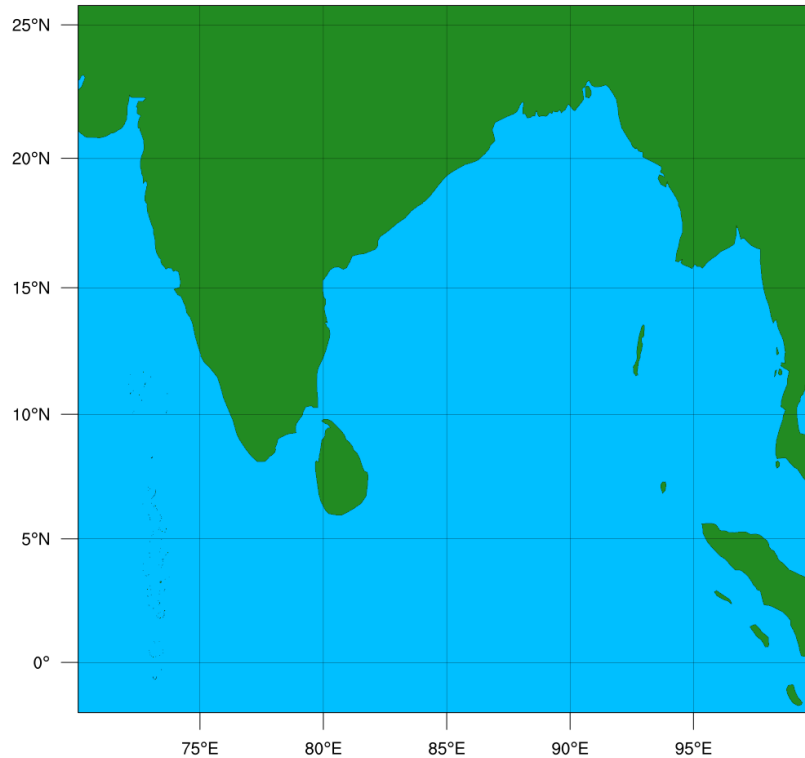


Figure S2: Study domain over the BoB for cyclone Nivar.

S2 Comparison of different initialization and input forcings

20 The results obtained from the model simulations with two input forcings, FNL and GFS, initialized for three initial conditions at an interval of 6-hours are presented here. Model simulated tracks of TCs, MSW and MSLP are described. The CT, AT, MSW, and MSLP errors for all the simulations are evaluated and compared with IMD best-track data.

2.1 For TC's track prediction

25 Figure S3 depicts the simulated tracks of cyclones Tauktae and Nivar from all experiments, as well as the IMD best-track (a-b). The initial vortex of the cyclone Tauktae was formed on the west side of the actual location in most experiments using GFS and FNL forcing simulations with different initializations. Before making landfall, the cyclone moved northward with slight deflection to north-westward, followed by northeast propagation. The simulated tracks shifted towards the left of the observed track. This can be attributed to the WRF model's inherent
30 bias for northwest moving cyclones (Srinivas et al., 2013). The impact of the forcing datasets was minor on Tauktae's track; however, those with the FNL forcings were slightly closer to the observed track. The 06 UTC 14 May initialization (14_06) and FNL forcing have produced a better track than others for Tauktae. In comparison to the Tauktae, the simulated tracks for cyclone Nivar (Fig. S3(b)) appear to be widely distributed. The effect of forcing datasets is found to be smaller than that of various initializations, i.e., the track prediction of cyclone Nivar
35 over the study region is more sensitive to initializations than GFS and FNL forcings.

Further, we computed the AT (Fig. S4) and CT error (Fig. S5) for both the cases and for all the simulations. For cyclone Tauktae, all the experiments showed a tendency of running behind the observation (Fig. S4(a)). Experiment 14_06 performed best with the least error for both the forcings even though it had the larger error at the start of the simulation; however, the AT error was reduced by approximately 4% from GFS to FNL. On the other hand, in the case of cyclone Nivar, GFS forcings showed relatively lesser AT error for all the experiments (Fig. S4(b)). Overall, the model has performed well up to landfall for both cases, whereas larger AT errors can be seen after 6-12 hours of the landfall time.

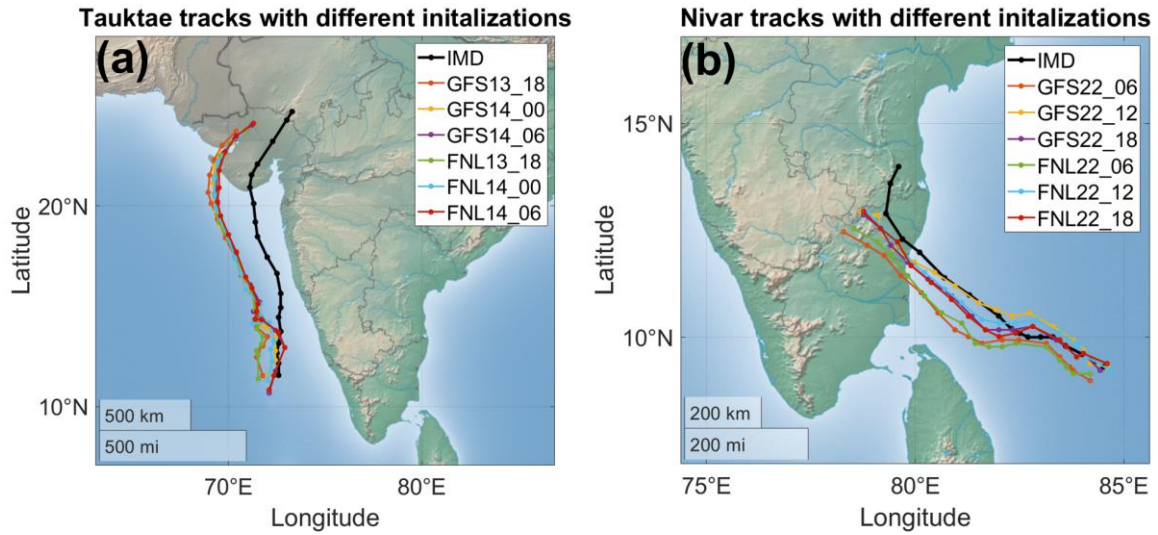


Figure S3: Simulated tracks of a) ESCS Tauktae and b) VSCS Nivar from two input forcings GFS and FNL initialized from three different initial conditions. Observed tracks of both TCs are obtained from IMD best-track data.

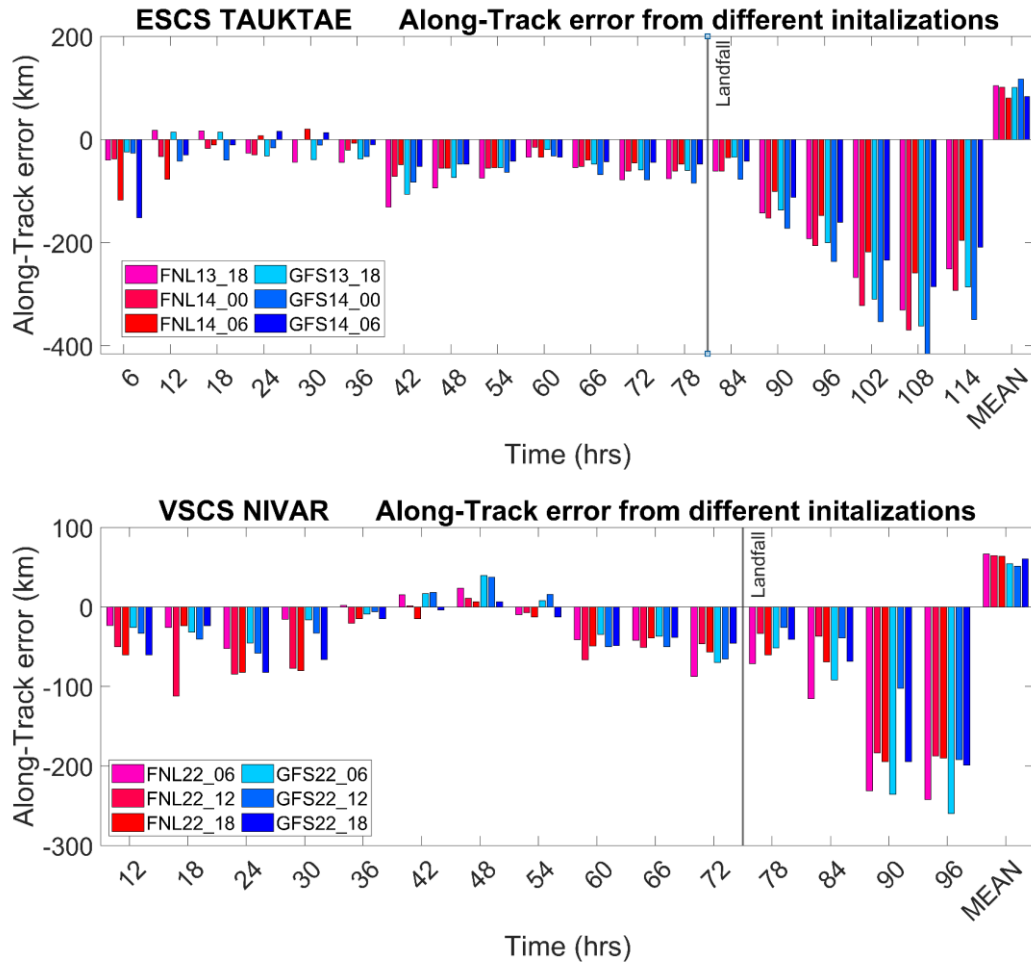


Figure S4: Along track error (km) for the simulated tracks of a) ESCS Tauktae and b) VSCS Nivar from two input forcings GFS and FNL initialized from three different initial conditions.

During the initial hours (6-24) of the cyclone Tauktae, model experiments showed a smaller CT error (Fig. S5(a)). Except at the 18-hour integration time for 14_06 experiments with FNL and GFS forcings, the CT error was negative throughout the simulations. A gradual increase was found from the 30-hour integration time step up to 84-hour. Overall performance of the model was better for the 14_06 experiment with FNL forcing. On the other hand, in the case of cyclone Nivar, the experiments show varying results (Fig. S5(b)). In some case GFS performed better and other FNL and the 22_06 experiment performed worst, and the other two are close to each other.

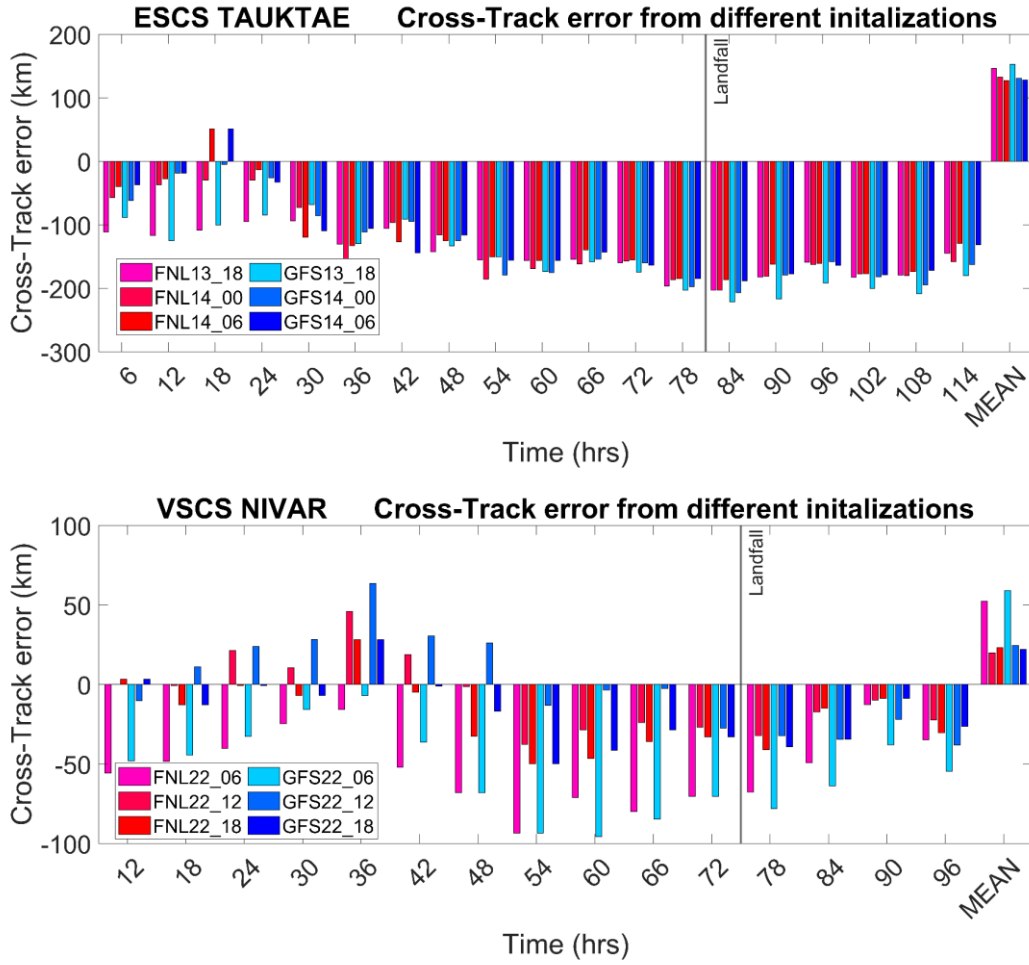


Figure S5: Cross-track error (km) for the simulated tracks of a) ESCS Tauktae and b) VSCS Nivar from two input forcings GFS and FNL initialized from three different initial conditions.

S2.2 For TC's intensity prediction

For ESCS Tauktae MSW (Fig. S6(a)), the model experiments captured the peak value accurately even though the decay pattern was not captured as seen in observation. All the simulations showed an overestimation in the intensity till 60 hours. Between 60 to 78 hours, the simulations underestimated the MSW and then again started to overestimate.

In the case of VSCS Nivar, we can see the experiments captured the pattern with overestimation throughout the timeseries analysis, as seen in Figure S6(b). At the start, the model simulations are further away from the observation and with time progression the error seems to reduce by quite some margin. The spread among the different simulations is low at 66-hour mark suggesting all the experiments have well captured the intensity during landfall.

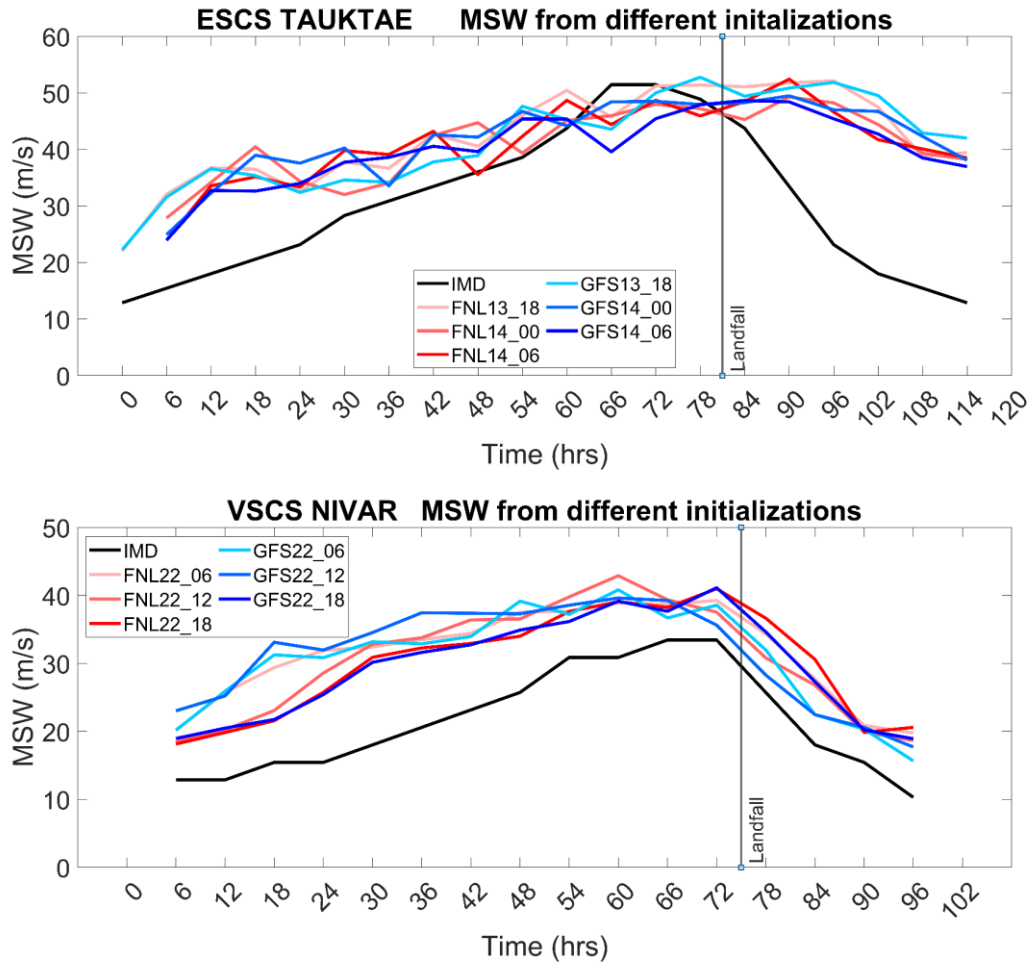


Figure S6: MSW time series at 6-hour intervals for the simulated tracks of a) ESCS Tauktae and b) VSCS Nivar from two input forcings GFS and FNL initialized from three different initial conditions.

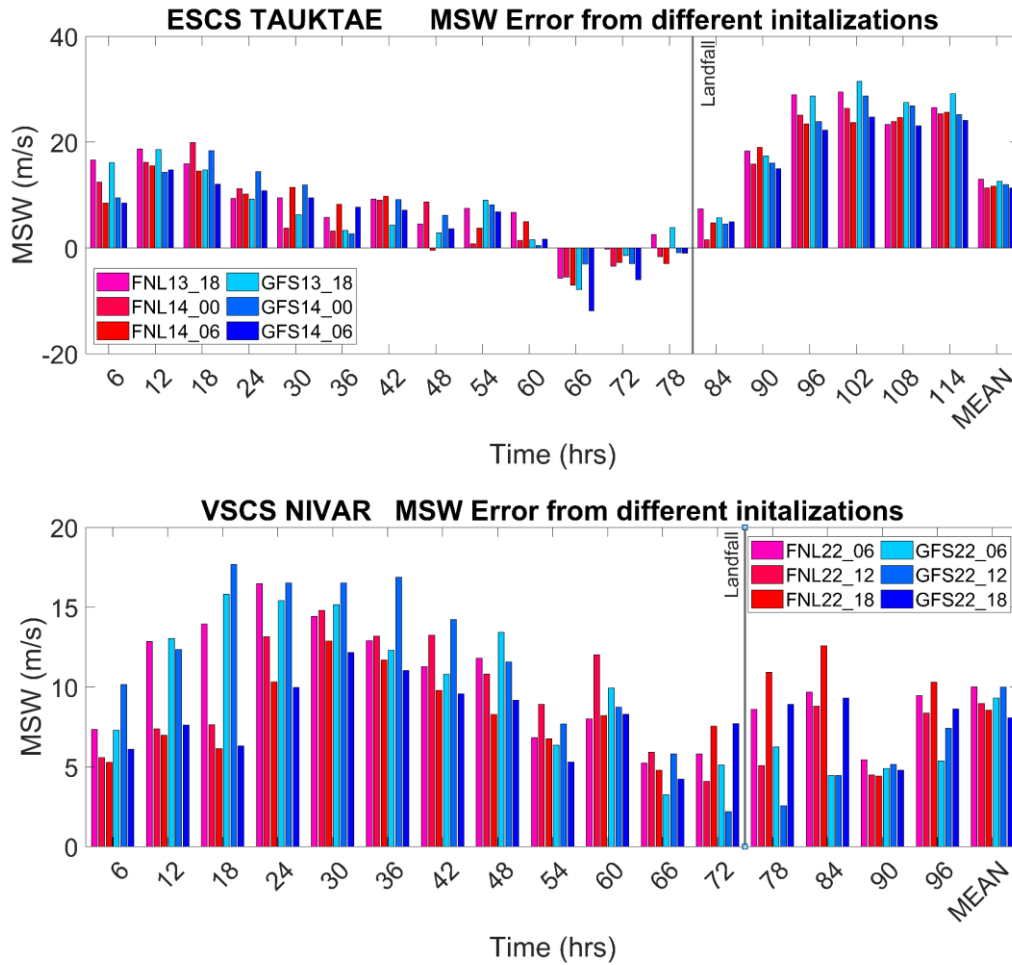


Figure S7: MSW error at 6-hour intervals for the simulated tracks of a) ESCS Tauktae and b) VSCS Nivar from two input forcings GFS and FNL initialized from three different initial conditions.

Subtracting the simulated MSW obtained from the different experiments from IMD best-track data given us the error in MSW. The MSW error in the case of ESCS Tauktae decreased from the start approaching the observed values but increased back again after the landfall (Fig. S7(a)). Near the landfall time at 78-hour, the error was in close proximity to IMD reported values for many experiments. Overall, the difference in all the experiments was very less. For VSCS Nivar, the MSW error stayed positive throughout, suggesting overestimation in all the simulations and each simulation having a slightly different pattern (Fig. S7(b)). The error increased from start till 24-hours then decrease until landfall (66-hours) then increased back again. Overall, the MSW error was the least for the 22_18 experiment for both the forcings.

6-hourly time evolution of MSLP for the two cases is provided in Figure S8. In the case of Tauktae, we can see the model have overestimates throughout except for a couple of experiments where it crossed the observation time-series, and the peak intensity is delayed by 12-18 hours compared to observation (Fig. S8(a)). Same pattern was also observed for Tauktae's MSW time evolution analysis. On the other hand, for VSCS Nivar, all the experiments overestimated the MSLP at all time step (Fig. S8(b)); however, the model was able to capture the pattern. For both the forcings, 22_18 experiments have better captured the timing of peak intensity (lowest MSLP) compared with IMD reported data around 66-72 hours.

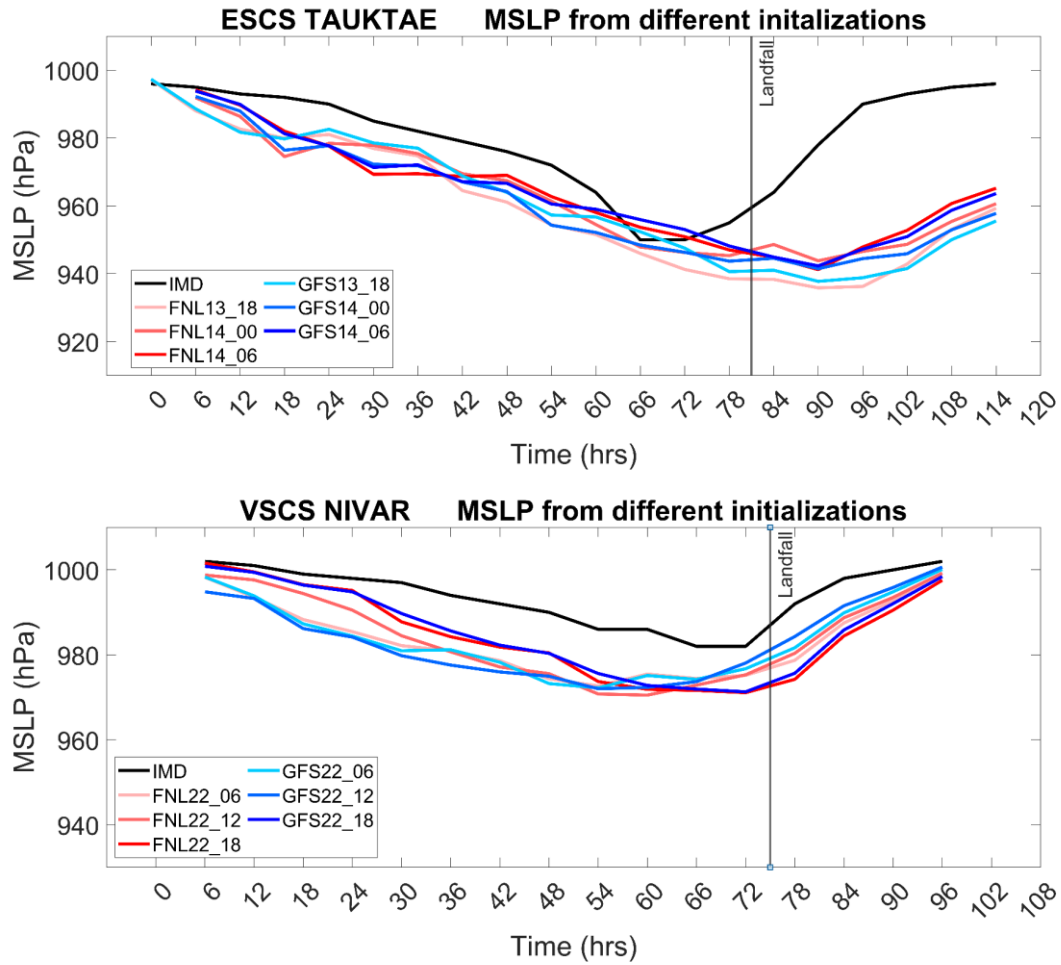


Figure S8: MSLP time series at 6-hour intervals for the simulated tracks of a) ESCS Tauktae and b) VSCS Nivar from two input forcings GFS and FNL initialized from three different initial conditions.

80 Subtracting the simulated MSLP from observed data gives the error in MSLP. The MSLP error for ESCS Tauktae was consistent until the landfall with couple simulation that deviated at 66-72 hours (Fig. S9(a)). After the landfall, the error increased drastically in all the experiments. The 14_06 experiment with FNL forcing had least error. For VSCS Nivar, the error varied significantly among the experiments but stayed consistent even after the landfall (Fig. S9(b)). At 66 and 72 hours, which is around the landfall period, the error was comparatively less. Overall,

85 the experiments with last initialization time (22_18) performed better for both the TCs with both forcing.

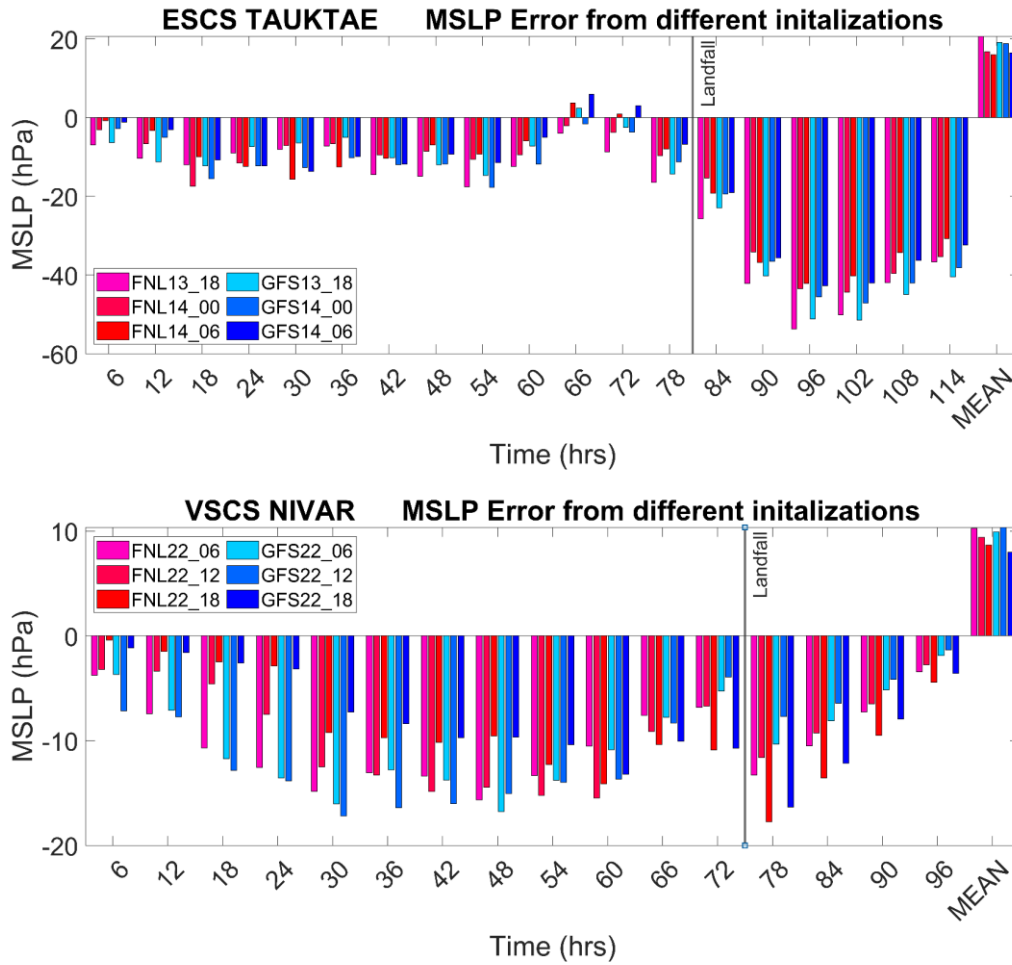


Figure S9: MSLP error at 6-hour intervals for the simulated tracks of a) ESCS Tauktae and b) VSCS Nivar from two input forcings GFS and FNL initialized from three different initial conditions.

S2.3 Error statistics for TC's track and intensity prediction

Tables S1 and S2 are constructed by taking the absolute mean of each error term for all the experiments and averaging them accordingly. So, we have a table with statistics of average CT, AT, MSW, and MSLP errors for three initialization and two forcing for both TC cases. Tables show that the average CT error was lowest when the FNL forcings were used, whereas AT error was minimum with FNL forcing for ESCS Tauktae and GFS forcing for VSCS Nivar. The MSW and MSLP error for both the forcing were close to each other, and we see the significant difference only in MSLP error for ESCS Tauktae, where FNL forcing performed better. The errors homogeneously decrease as we get closer to the mature stage of the cyclone. Overall, we can conclude that FNL forcing performed better than GFS. Therefore, for further analysis, FNL forcing with initialization time 14_06 and 22_18 was used for ESCS Tauktae and VSCS Nivar, respectively.

ESCS Tauktae

Initialization Time	CT Error (km)		AT Error (km)		MSW Error (m/s)		MSLP Error (hPa)	
	GFS	FNL	GFS	FNL	GFS	FNL	GFS	FNL
13_18	152.6	146.2	100.6	104.2	12.6	13.0	19.1	20.7
14_00	130.5	132.4	117.4	100.9	12.0	11.3	18.8	16.8
14_06	128.0	127.0	83.6	80.2	11.3	11.6	16.4	16.0
Mean	137.0	135.2	100.5	95.1	12.0	12.0	18.1	17.8

Table S1 Average error statistics for ESCS Tauktae.

100

VSCS Nivar								
Initialization Time	CT Error (km)		AT Error (km)		MSW Error (m/s)		MSLP Error (hPa)	
	GFS	FNL	GFS	FNL	GFS	FNL	GFS	FNL
22_06	58.9	52.3	54.5	66.6	9.3	10.0	9.9	10.3
22_12	24.5	19.8	51.2	64.6	10.0	9.0	10.4	9.4
22_18	22.1	23.3	60.4	63.6	8.1	8.6	8.0	8.7
Mean	35.2	31.8	55.4	64.9	9.1	9.2	9.4	9.4

Table S2 Average error statistics for VSCS Nivar.

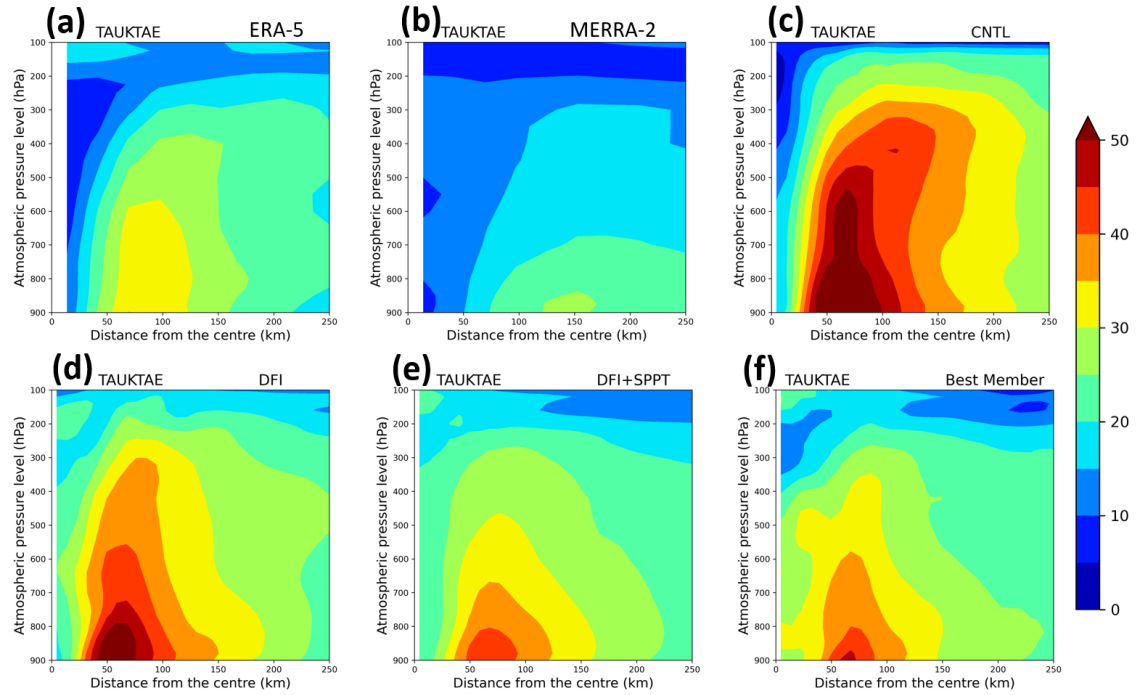


Figure S10: Vertically distributed azimuthally averaged wind speed for Tauktae at the time of maximum intensity from the two reanalysis datasets a) ERA-5 & b) MERRA-2, and from the experiments c) CNTL, d) DFI, e) DFI+SPPT, and d) Best Member simulations. The maximum intensity (MSW) and TC's centre location were taken from IMD best-track data for the reanalysis products. At the same time, for the model simulations, both attributes correspond to the particular experiment.

Figure S10 depicts the vertically averaged azimuthally averaged wind distribution for Tauktae from observations (reanalysis products) and model simulations. Clearly, the observations (Fig. S10a-b) did not justify capturing the wind magnitude of a cyclonic system; however, the wind patterns were more or less similar among observations as well as simulations. The maximum wind was centred between 50 to 100 km distance from the storm's centre. As seen from Fig. S10c, the CNTL experiment exhibited stronger contours (> 35 m/s) from the lower troposphere up to 300 hPa. These patterns were weaker in the DFI (Fig. S10d), DFI+SPPT (Fig. S10e), and Best Member (Fig. S10f) experiments. In the same way, the CNTL experiment produced maximum intensity of the cyclone Tauktae, followed by other experiments, respectively. A similar kind of wind distribution as well as magnitude were found in the case of Nivar also (Fig. S11).

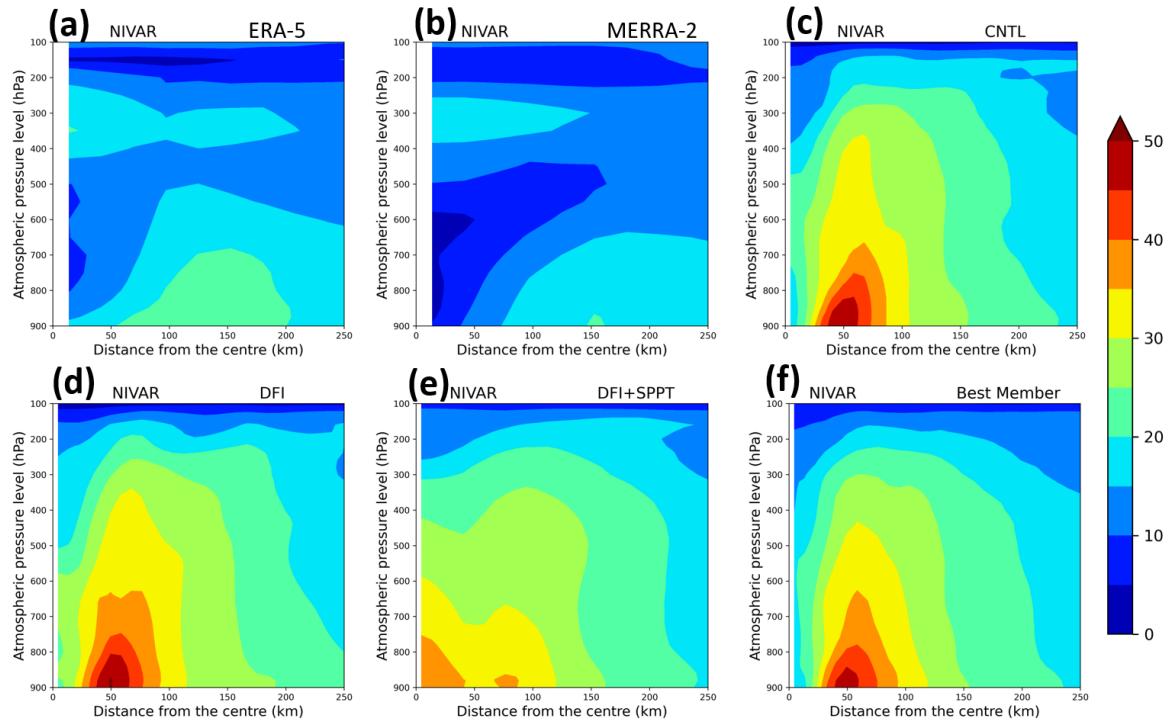


Figure S11: Same as Figure S10 but for Nivar.